VIETNAM ACADEMY OF SCIENCE AND TECHNOLOGY

Vietnam Journal of MECHANICS

Volume 35 Number 4

ISSN 0866-7136

VN INDEX 12.666

4

2013

35th Anniversary

Vietnam Journal of Mechanics, VAST, Vol. 35, No. 4 (2013), pp. 285 – 298

NONLINEAR BUCKLING AND POST-BUCKLING OF ECCENTRICALLY STIFFENED FUNCTIONALLY GRADED CYLINDRICAL SHELLS SURROUNDED BY AN ELASTIC MEDIUM BASED ON THE FIRST ORDER SHEAR DEFORMATION THEORY

Dao Van Dung*, Nguyen Thi Nga
Hanoi University of Science, VNU, Vietnam
*E-mail: dungdv90@gmail.com

Abstract. In this paper, the nonlinear buckling and post-buckling of an eccentrically stiffened cylindrical shell made of functionally graded materials, surrounded by an elastic medium and subjected to mechanical compressive loads and external pressures are investigated by an analytical approach. The cylindrical shells are reinforced by longitudinal and circumferential stiffeners. The material properties of cylindrical shells are graded in the thickness direction according to a volume fraction power-law distribution. The nonlinear stability equations for stiffened cylindrical shells are derived by using the first order shear deformation theory and smeared stiffeners technique. Closed-form expressions for determining the buckling load and load-deflection curves are obtained. The effectiveness of stiffeners in enhancing the stability of cylindrical shells is shown. The effects of volume fraction indexes, material properties, geometrical parameters and foundation parameters are analyzed in detail.

Keywords: Stiffened cylindrical shells, nonlinear buckling and post-buckling, functionally graded, foundations.

1. INTRODUCTION

Functionally graded material (FGM) cylindrical shells in recent years, are extensively used in many modern engineering applications. These structures are usually rested on or placed in a soil medium modelled as an elastic foundation. Thus, their stability analysis is an important problem and has received considerable interest by researchers. Bagherizadeh et al. [1] investigated the mechanical buckling of FGM cylindrical shell surrounded by Pasternak elastic foundation and subjected to combined axial and radial compressive loads based on a higher-order shear deformation shell theory (HSDT). The elastic foundation is modelled by two-parameter Pasternak model, which is obtained by adding a shear layer to the Winkler model. Shen and Wang [2] presented thermal buckling and post-buckling behavior for fiber reinforced composite (FRC) laminated cylindrical shells embedded in a large outer elastic medium and subjected to a uniform temperature rise. The surrounding elastic medium is modeled as a Pasternak foundation. Shen [3] presented the post-buckling response of a shear deformable functionally graded (FG) cylindrical shell of finite length embedded in a large outer elastic medium and subjected to axial compressive loads in thermal environments based on a higher order shear deformation shell theory with von Kármán–Donnell-type of kinematic nonlinearity. Shen et al. [4] studied post-buckling of internal pressure loaded FG cylindrical shells surrounded by an elastic medium. This work employed a higher order shear deformation shell theory with von Kármán–Donnell-type of kinematic nonlinearity and a singular perturbation technique. Sofiyev and Kuruoglu [5] investigated torsional vibration and buckling of the cylindrical shell with functionally graded coatings surrounded by an elastic medium.

Recently, idea of eccentrically stiffened FGM structures has been proposed by Bich et al. [6–8] and Najafizadeh et al. [9]. Bich et al. [6–8] studied the nonlinear static buckling behavior of eccentrically stiffened imperfect FGM plates and shallow shells and the nonlinear dynamic response of eccentrically stiffened FGM imperfect panels and doubly curved thin shallow shells on the basis of the classical plate and shell theory. Stiffeners are assumed to be homogenous. By considering FGM stiffeners, Najafizadeh et al. [9] investigated the mechanical buckling behavior of axially loaded FGM stiffened cylindrical shells reinforced by rings and stringers based on the classical shell theory (CST). Following this direction, Dung and Hoa [10, 11] researched on nonlinear buckling and post-buckling of eccentrically stiffened FGM thin circular cylindrical shells under torsional load or external pressure. Approximate three-term solution of deflection taking into account the nonlinear buckling shape is chosen and the Galerkin method is used in those works.

In this paper, following the direction of work [6–8], the nonlinear buckling and post-buckling analysis of eccentrically stiffened FGM thin circular cylindrical shells surrounded by an elastic medium and under axial load and external pressure based on the first order shear deformation theory (FSDT) is studied. Governing equations using the smeared stiffeners technique and FSDT are derived. Applying Galerkin's method, the closed-form expression to determine the buckling loads and post-buckling equilibrium paths are found. The effects of various parameters as stiffeners and foundations, volume fraction index of material and geometrical parameters on the nonlinear stability of cylindrical shells are shown.

2. FUNCTIONALLY GRADED SHELLS AND THEORETICAL FORMULATIONS

2.1. Functionally graded material shells

Consider a functionally graded material cylindrical shell of length L, mean radius R, and uniform thickness h, as depicted in Fig. 1. An orthogonal Descartes coordinate system xyz is chosen so that the axes $x, y\,(y = R\theta)$ are in the longitudinal, circumferential directions, respectively, and the axis z is perpendicular to the middle surface and in inward thickness direction $\left(-\dfrac{h}{2} \le z \le \dfrac{h}{2}\right)$.

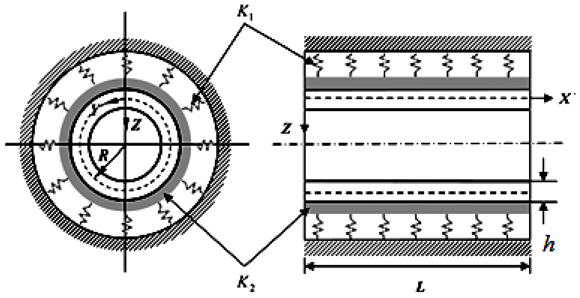

Fig. 1. Configuration of a cylindrical shell surrounded by an elastic medium

The cylindrical shell is assumed to be made from a mixture of ceramic and metal with the volume-fractions given by a power-law distribution as

$$V_m + V_c = 1, V_c = V_c(z) = \left(\frac{z}{h} + \frac{1}{2}\right)^k, \tag{1}$$

where k is the volume fraction exponent and takes only non-negative values, and the subscripts m and c refer to the metal and ceramic constituents, respectively. According to the mixture rule, the effective Young's modulus can be expressed by

$$E = E(z) = E_m V_m + E_c V_c = E_m + (E_c - E_m)\left(\frac{z}{h} + \frac{1}{2}\right)^k \tag{2}$$

whereas the Poisson's ratio is assumed to be a constant. As can be seen, from Eq. (2) that, the surface $\left(z = \frac{h}{2}\right)$ of a cylindrical shell is ceramic-rich whereas the surface $\left(z = -\frac{h}{2}\right)$ is metal-rich.

2.2. Theoretical formulations

Using the first order shear deformation shell theory and geometrical nonlinearity in von Karman sense, the strains across the cylindrical shell thickness at a distance z from the middle surface are [12]

$$\begin{bmatrix} \varepsilon_x \\ \varepsilon_y \\ \gamma_{xy} \end{bmatrix} = \begin{bmatrix} \varepsilon_x^0 \\ \varepsilon_y^0 \\ \gamma_{xy}^0 \end{bmatrix} + z \begin{bmatrix} \kappa_x \\ \kappa_y \\ \kappa_{xy} \end{bmatrix}, \tag{3}$$

$$\begin{bmatrix} \gamma_{xz} \\ \gamma_{yz} \end{bmatrix} = \begin{bmatrix} \gamma_{xz}^0 \\ \gamma_{yz}^0 \end{bmatrix} = \begin{bmatrix} w_{,x} + \phi_x \\ w_{,y} + \phi_y \end{bmatrix}, \tag{4}$$

where

$$\begin{bmatrix} \varepsilon_x^0 \\ \varepsilon_y^0 \\ \gamma_{xy}^0 \end{bmatrix} = \begin{bmatrix} u_{,x} + \frac{1}{2} w_{,x}^2 \\ v_{,y} + \frac{1}{2} w_{,y}^2 - \frac{w}{R} \\ u_{,y} + v_{,x} + w_{,x} w_{,y} \end{bmatrix}, \begin{bmatrix} \kappa_x \\ \kappa_y \\ \kappa_{xy} \end{bmatrix} = \begin{bmatrix} \phi_{x,x} \\ \phi_{y,y} \\ \phi_{x,y} + \phi_{y,x} \end{bmatrix}, \tag{5}$$

in which ε_x, ε_y are normal strains, γ_{xy} is the in-plane shear strain and γ_{xz}, γ_{yz} are the transverse shear deformations. Also, u, v, w are the displacement components along the x, y, z directions, respectively, and ϕ_x, ϕ_y are the slope rotation in the (y, z) and (x, z) planes, respectively. From the relations (5), the compatibility equation of a cylindrical shell is obtained as

$$\varepsilon^0_{x,yy} + \varepsilon^0_{y,xx} - \gamma^0_{xy,xy} = w^2_{,xy} - w_{,xx}w_{,yy} - \frac{1}{R}w_{,xx}. \tag{6}$$

Assume that the cylindrical shell and stiffeners are treated as assembled shell and beams elements and shell is reinforced by closely spaced [13] homogeneous ring and stringer stiffener systems. Stiffener is pure-ceramic if it is located at ceramic-rich side and is pure-metal if is located at metal-rich side, and such FGM stiffened circular cylindrical shells provide continuity between shells and stiffeners. In this case, the stress-strain relationship is given by Hooke's law as,

for shells

$$\left(\sigma^{sh}_x, \sigma^{sh}_y\right) = \frac{E(z)}{1-\nu^2}\left[(\varepsilon_x, \varepsilon_y) + \nu\left(\varepsilon_y, \varepsilon_x\right)\right], \left(\sigma^{sh}_{xy}, \sigma^{sh}_{xz}, \sigma^{sh}_{yz}\right) = \frac{E(z)}{2\left(1+\nu\right)}\left(\gamma_{xy}, \gamma_{xz}, \gamma_{yz}\right), \tag{7}$$

and for stiffeners [14]

$$\begin{aligned} \sigma^s_x &= E_{sx}\varepsilon_x, & \sigma^s_y &= E_{sy}\varepsilon_y, \\ \sigma^s_{xz} &= G_{sx}\gamma_{xz}, & \sigma^s_{yz} &= G_{sy}\gamma_{yz}. \end{aligned} \tag{8}$$

where the superscripts "*sh*" and "*s*" denote shell and stiffener, respectively; E_{sx}, E_{sy} and G_{sx}, G_{sy} are Young's moduli and shear moduli of longitudinal and circumferential stiffeners, respectively.

Taking into account the contribution of stiffeners by the smeared stiffeners technique and omitting the twist of stiffeners and integrating the above stress-strain equations and their moments through the thickness of the cylindrical shell, we obtain the expressions for force and moment resultants of an eccentrically stiffened FGM cylindrical shell

$$\begin{aligned} N_x &= \left(A_{11} + \frac{E_{sx}A_1}{d_1}\right)\varepsilon^0_x + A_{12}\varepsilon^0_y + \left(B_{11} + C_1\right)\phi_{x,x} + B_{12}\phi_{y,y}, \\ N_y &= A_{12}\varepsilon^0_x + \left(A_{22} + \frac{E_{sy}A_2}{d_2}\right)\varepsilon^0_y + B_{12}\phi_{x,x} + \left(B_{22} + C_2\right)\phi_{y,y}, \\ N_{xy} &= A_{66}\gamma^0_{xy} + B_{66}\left(\phi_{x,y} + \phi_{y,x}\right), \end{aligned} \tag{9}$$

$$\begin{aligned} M_x &= \left(B_{11} + C_1\right)\varepsilon^0_x + B_{12}\varepsilon^0_y + \left(D_{11} + \frac{E_{sx}I_1}{d_1}\right)\phi_{x,x} + D_{12}\phi_{y,y}, \\ M_y &= B_{12}\varepsilon^0_x + \left(B_{22} + C_2\right)\varepsilon^0_y + \left(D_{22} + \frac{E_{sy}I_2}{d_2}\right)\phi_{y,y} + D_{12}\phi_{x,x}, \\ M_{xy} &= B_{66}\gamma^0_{xy} + D_{66}\left(\phi_{x,y} + \phi_{y,x}\right). \end{aligned} \tag{10}$$

The transverse shear force resultants are

$$Q_x = A_{44}w_{,x} + A_{44}\phi_x, \quad Q_y = A_{55}w_{,y} + A_{55}\phi_y, \tag{11}$$

where the specific expressions of coefficients A_{ij}, B_{ij}, D_{ij} are given as

$$\begin{aligned}
&A_{11} = A_{22} = \frac{E_1}{1-\nu^2}, && A_{12} = \frac{E_1\nu}{1-\nu^2}, && A_{66} = \frac{E_1}{2(1+\nu)},\\
&A_{44} = \chi_1\left[\frac{E_1}{2(1+\nu)} + \frac{G_{sx}A_1}{d_1}\right], && A_{55} = \chi_2\left[\frac{E_1}{2(1+\nu)} + \frac{G_{sy}A_2}{d_2}\right], && \\
&B_{11} = B_{22} = \frac{E_2}{1-\nu^2}, && B_{12} = \frac{E_2\nu}{1-\nu^2}, && B_{66} = \frac{E_2}{2(1+\nu)},\\
&D_{11} = D_{22} = \frac{E_3}{1-\nu^2}, && D_{12} = \frac{E_3\nu}{1-\nu^2}, && D_{66} = \frac{E_3}{2(1+\nu)},
\end{aligned} \tag{12}$$

and

$$\begin{aligned}
&E_1 = \left(E_m + \frac{E_c - E_m}{k+1}\right)h, \quad E_2 = \frac{(E_c - E_m)\,kh^2}{2(k+1)(k+2)},\\
&E_3 = \left[\frac{E_m}{12} + (E_c - E_m)\left(\frac{1}{k+3} - \frac{1}{k+2} + \frac{1}{4k+4}\right)\right]h^3,
\end{aligned} \tag{13}$$

and

$$\begin{aligned}
&I_1 = \frac{b_1h_1^3}{12} + A_1e_1^2, && I_2 = \frac{b_2h_2^3}{12} + A_2e_2^2,\\
&C_1 = \pm\frac{E_{sx}A_1e_1}{d_1}, && C_2 = \pm\frac{E_{sy}A_2e_2}{d_2},\\
&e_1 = \frac{h_1 + h}{2}, && e_2 = \frac{h_2 + h}{2}.
\end{aligned} \tag{14}$$

In the relation (12), χ_1 and χ_2 are the shear correction factors and are taken as $\chi_1 = \chi_2 = 5/6$. Note that Young's modulus of stiffener takes the value being assigned to E_m if the full metal stiffeners are put at the metal-rich side of the cylindrical shell and conversely being assigned to E_c if the full ceramic ones at the ceramic-rich side. In addition, the thickness and width for longitudinal stiffeners (x-direction) are respectively denoted by h_1 and b_1 and for circumferential stiffeners (y-direction) are h_2 and b_2. Also, d_1 and d_2 are the distance between two longitudinal and circumferential stiffeners, respectively. The quantities A_1, A_2 are the cross-section areas of stiffeners and I_1, I_2 are the second moments of inertia of the stiffener cross sections relative to the cylindrical shell middle surface; and the eccentricities e_1 and e_2 represent the distance from the cylindrical shell middle surface to the centroid of the longitudinal and circumferential stiffener cross section, respectively. The quantities C_1 and C_2 are taken plus sign if stiffeners are attached inside and taken minus sign if they are outside.

The strain-force resultant relations reversely are obtained from Eq. (9)

$$\begin{aligned}
&\varepsilon_x^0 = A_{22}^*N_x - A_{12}^*N_y - B_{11}^*\phi_{x,x} - B_{12}^*\phi_{y,y},\\
&\varepsilon_y^0 = A_{11}^*N_y - A_{12}^*N_x - B_{21}^*\phi_{x,x} - B_{22}^*\phi_{y,y},\\
&\gamma_{xy}^0 = A_{66}^*N_{xy} - B_{66}^*\left(\phi_{x,y} + \phi_{y,x}\right).
\end{aligned} \tag{15}$$

Substituting Eq. (15) into Eq. (10) yields

$$\begin{aligned}
&M_x = B_{11}^*N_x + B_{21}^*N_y + D_{11}^*\phi_{x,x} + D_{12}^*\phi_{y,y},\\
&M_y = B_{12}^*N_x + B_{22}^*N_y + D_{21}^*\phi_{x,x} + D_{22}^*\phi_{y,y},\\
&M_{xy} = B_{66}^*N_{xy} + D_{66}^*\left(\phi_{x,y} + \phi_{y,x}\right),
\end{aligned} \tag{16}$$

where the coefficients A^*_{ij}, B^*_{ij} and D^*_{ij} are found in Appendix I.

The nonlinear equilibrium equations of FGM cylindrical shells surrounded by an elastic medium, based on the first order shear deformation theory, are [1, 12]

$$N_{x,x} + N_{xy,y} = 0, \tag{17}$$

$$N_{xy,x} + N_{y,y} = 0, \tag{18}$$

$$Q_{x,x} + Q_{y,y} + N_x w_{,xx} + 2N_{xy} w_{,xy} + N_y w_{,yy} + q + \frac{1}{R} N_y - K_1 w + K_2 \left(w_{,xx} + w_{,yy}\right) = 0, \tag{19}$$

$$M_{x,x} + M_{xy,y} - Q_x = 0, \tag{20}$$

$$M_{xy,x} + M_{y,y} - Q_y = 0. \tag{21}$$

where K_1 (N/m^3) is modulus of subgrade reaction for foundation and K_2 (N/m)-the shear modulus of the subgrade and q is uniform lateral pressure. Introduce Airy's stress function $f = f(x, y)$ so that

$$N_x = f_{,yy}, \quad N_y = f_{,xx}, \quad N_{xy} = -f_{,xy}. \tag{22}$$

It is easy to see that the first two equations (17) and (18) are automatically satisfied. Three equations (19), (20) and (21) become

$$\begin{aligned} & M_{x,xx} + 2M_{xy,xy} + M_{y,yy} + f_{,yy} w_{,xx} - 2f_{,xy} w_{,xy} + f_{,xx} w_{,yy} + \\ & \qquad + q + \frac{1}{R} N_y - K_1 w + K_2 \left(w_{,xx} + w_{,yy}\right) = 0, \\ & M_{x,x} + M_{xy,y} - Q_x = 0, \\ & M_{xy,x} + M_{y,y} - Q_y = 0. \end{aligned} \tag{23}$$

Substituting the expressions of M_{ij} in Eq. (16) and Q_x, Q_y in Eq. (11) into Eq. (23), we obtain

$$\begin{aligned} \Omega \equiv\, & B^*_{21} \frac{\partial^4 f}{\partial x^4} + \left(B^*_{11} + B^*_{22} - 2B^*_{66}\right) \frac{\partial^4 f}{\partial x^2 \partial y^2} + B^*_{12} \frac{\partial^4 f}{\partial y^4} + D^*_{11} \frac{\partial^3 \phi_x}{\partial x^3} + \\ & + \left(D^*_{12} + 2D^*_{66}\right) \frac{\partial^3 \phi_y}{\partial x^2 \partial y} + \left(D^*_{21} + 2D^*_{66}\right) \frac{\partial^3 \phi_x}{\partial x \partial y^2} + D^*_{22} \frac{\partial^3 \phi_y}{\partial y^3} + \frac{\partial^2 f}{\partial y^2} \frac{\partial^2 w}{\partial x^2} - \\ & - 2 \frac{\partial^2 f}{\partial x \partial y} \frac{\partial^2 w}{\partial x \partial y} + \frac{\partial^2 f}{\partial x^2} \frac{\partial^2 w}{\partial y^2} + q + \frac{1}{R} \frac{\partial^2 f}{\partial x^2} - K_1 w + K_2 \left(\frac{\partial^2 w}{\partial x^2} + \frac{\partial^2 w}{\partial y^2}\right) = 0, \end{aligned} \tag{24}$$

$$B^*_{21} \frac{\partial^3 f}{\partial x^3} + \left(B^*_{11} - B^*_{66}\right) \frac{\partial^3 f}{\partial x \partial y^2} + D^*_{11} \frac{\partial^2 \phi_x}{\partial x^2} + \left(D^*_{12} + D^*_{66}\right) \frac{\partial^2 \phi_y}{\partial x \partial y} + D^*_{66} \frac{\partial^2 \phi_x}{\partial y^2} - A_{44} \frac{\partial w}{\partial x} - A_{44} \phi_x = 0, \tag{25}$$

$$B^*_{12} \frac{\partial^3 f}{\partial y^3} + \left(B^*_{22} - B^*_{66}\right) \frac{\partial^3 f}{\partial y \partial x^2} + D^*_{22} \frac{\partial^2 \phi_y}{\partial y^2} + \left(D^*_{21} + D^*_{66}\right) \frac{\partial^2 \phi_x}{\partial x \partial y} + D^*_{66} \frac{\partial^2 \phi_y}{\partial x^2} - A_{55} \frac{\partial w}{\partial y} - A_{55} \phi_y = 0. \tag{26}$$

The system of Eqs. (24) $\div$ (26) includes four unknown functions w, ϕ_x, ϕ_y and f so it is necessary to find the fourth equation relating to these functions by using the compatibility equation (6). For this aim, substituting the expressions of ε_{ij} in Eq. (15) into Eq. (6), one can write as

$$\begin{aligned} & A_{11}^{*} \frac{\partial^4 f}{\partial x^4} + \left(A_{66}^{*} - 2A_{12}^{*}\right) \frac{\partial^4 f}{\partial x^2 \partial y^2} + A_{22}^{*} \frac{\partial^4 f}{\partial y^4} - B_{21}^{*} \frac{\partial^3 \phi_x}{\partial x^3} - \left(B_{11}^{*} - B_{66}^{*}\right) \frac{\partial^3 \phi_x}{\partial x \partial y^2} - \\ & \quad - \left(B_{22}^{*} - B_{66}^{*}\right) \frac{\partial^3 \phi_y}{\partial y \partial x^2} - B_{12}^{*} \frac{\partial^3 \phi_y}{\partial y^3} - \left(\frac{\partial^2 w}{\partial x \partial y}\right)^2 + \frac{\partial^2 w}{\partial x^2} \frac{\partial^2 w}{\partial y^2} + \frac{1}{R} \frac{\partial^2 w}{\partial x^2} = 0. \end{aligned} \tag{27}$$

Eqs. (24) ÷ (27) are nonlinear equations in terms of four dependent unknown functions w, ϕ_x, ϕ_y and f and are used to investigate the stability of eccentrically stiffened functionally graded (ES-FGM) cylindrical shells surrounded by an elastic medium and under mechanical loads.

3. BUCKLING AND POST-BUCKLING ANALYSIS

Assume that an ES-FGM cylindrical shell is simply supported at $x = 0, x = L$ and subjected to in-plane compression load uniformly distributed of intensities P_x along x-direction and uniform lateral pressure q. Thus the boundary conditions are given by

$$w = \phi_y = N_{xy} = M_x = 0, \quad N_x = N_{x0} = -hP_x \quad \text{at} \quad x = 0, x = L. \tag{28}$$

The approximate solution of the system of Eqs. (24) ÷ (27) satisfying the boundary conditions (28) can be expressed by

$$\begin{aligned} & w = W \sin \alpha x \sin \beta y, \\ & \phi_x = \phi_{10} \cos \alpha x \sin \beta y + \phi_{11} \sin 2\alpha x, \\ & \phi_y = \phi_{20} \sin \alpha x \cos \beta y + \phi_{21} \sin 2\beta y, \\ & f = f_1 \cos 2\alpha x + f_2 \cos 2\beta y + f_3 \sin \alpha x \sin \beta y + \frac{1}{2} N_{x0} y^2, \end{aligned} \tag{29}$$

where $\alpha = \dfrac{m\pi}{L}, \beta = \dfrac{n}{R}$ and m is number of half waves in x-direction and n is number of wave in y-direction, respectively.

Substituting Eq. (29) into Eqs. (25), (26) and (27) and carrying out some calculations, yield

$$\begin{aligned} & f_1 = \frac{4\alpha^2 D_{11}^{*} + A_{44}}{A_{11}^{*}\left(4\alpha^2 D_{11}^{*} + A_{44}\right) + 4\alpha^2 B_{21}^{*2}} \cdot \frac{\beta^2}{32\alpha^2} W^2 = L_1.W^2, \\ & f_2 = \frac{4\beta^2 D_{22}^{*} + A_{55}}{A_{22}^{*}\left(4\beta^2 D_{22}^{*} + A_{55}\right) + 4\beta^2 B_{12}^{*2}} \cdot \frac{\alpha^2}{32\beta^2} W^2 = L_2.W^2, \\ & f_3 = \frac{\left(A_{44} a_{22} \alpha - A_{55} a_{12} \beta\right) a_{13} + \left(A_{55} a_{11} \beta - A_{44} a_{21} \alpha\right) a_{23} + \dfrac{D^{*}}{R} \alpha^2}{D^{*}\left[\alpha^4 A_{11}^{*} + \alpha^2 \beta^2 \left(A_{66}^{*} - 2A_{12}^{*}\right) + \beta^4 A_{22}^{*}\right] + \left(a_{13} a_{22} - a_{12} a_{23}\right) a_{13} + \left(a_{11} a_{23} - a_{21} a_{13}\right) a_{23}} \cdot W \\ & \quad = L_3.W, \end{aligned} \tag{30}$$

and

$$\phi_{10} = L_4.W, \phi_{20} = L_5.W, \tag{31}$$

$$\phi_{11} = L_6.W^2, \phi_{21} = L_7.W^2, \tag{32}$$

where D^{*}, L_i are given in Appendix II.

Substituting the expression (29) into Eq. (24) and then applying Galerkin's method to the resulting equation

$$\int_0^{\pi R}\int_0^{L}\Omega\sin\frac{m\pi x}{L}\sin\frac{ny}{R}dxdy=0$$

yields

$$\begin{aligned}&\alpha^2\beta^2\left(L_1+L_2\right)\left(\frac{-L\pi R}{2}\right)\cdot W^3+\Big(16\alpha^4B_{21}^*L_1+16\beta^4B_{12}^*L_2-2\alpha^2\beta^2L_3-\frac{4\alpha^2}{R}L_1-8\alpha^3D_{11}^*L_6\\&\quad-8\beta^3D_{22}^*L_7\Big)\left(\frac{-4}{3\alpha\beta}\delta_m\delta_n\right)\cdot W^2+\left\{\left[\alpha^4B_{21}^*+\alpha^2\beta^2\left(B_{11}^*+B_{22}^*-2B_{66}^*\right)+\beta^4B_{12}^*-\frac{\alpha^2}{R}\right]L_3\right.\\&\quad+\left[\alpha^3D_{11}^*+\alpha\beta^2\left(D_{21}^*+2D_{66}^*\right)\right]L_4+\left[\beta^3D_{22}^*+\alpha^2\beta\left(D_{12}^*+2D_{66}^*\right)\right]L_5-\alpha^2N_{x0}\\&\quad\left.-K_1-\left(\alpha^2+\beta^2\right)K_2\right\}\left(\frac{L\pi R}{4}\right)\cdot W+q\left(\frac{4}{\alpha\beta}\delta_m\delta_n\right)=0\end{aligned}\tag{33}$$

in which $\delta_m=\dfrac{1-(-1)^m}{2},\delta_n=\dfrac{1-(-1)^n}{2}$.

Eq. (33) is governing equations used to determine critical buckling loads and post-buckling load-deflection curves of ES-FGM cylindrical shells surrounded by an elastic medium and subjected to mechanical compressive loads and external pressures.

If ES-FGM cylindrical shells only subjects to uniform external pressures $q, N_{x0}=0$ and m,n are odd numbers, thus Eq. (33) becomes

$$q=q(W)=\frac{I}{3}.W^3-J.W^2+K.W.\tag{34}$$

in which

$$\begin{aligned}&I=3\alpha^3\beta^3\left(L_1+L_2\right)\left(\frac{L\pi R}{8}\right),\\&J=-\frac{1}{3}\left(16\alpha^4B_{21}^*L_1+16\beta^4B_{12}^*L_2-2\alpha^2\beta^2L_3-\frac{4\alpha^2}{R}L_1-8\alpha^3D_{11}^*L_6-8\beta^3D_{22}^*L_7\right),\\&K=\left\{\left[\alpha^4B_{21}^*+\alpha^2\beta^2\left(B_{11}^*+B_{22}^*-2B_{66}^*\right)+\beta^4B_{12}^*-\frac{\alpha^2}{R}\right]L_3+\left[\alpha^3D_{11}^*+\alpha\beta^2\left(D_{21}^*+2D_{66}^*\right)\right]L_4\right.\\&\qquad\left.+\left[\beta^3D_{22}^*+\alpha^2\beta\left(D_{12}^*+2D_{66}^*\right)\right]L_5-K_1-\left(\alpha^2+\beta^2\right)K_2\right\}\left(\frac{-L\pi R\alpha\beta}{16}\right)\end{aligned}\tag{35}$$

Eq. (34) leads to the equation from which the upper and lower buckling external pressures may be obtained as

$$\begin{aligned}q_u=&\frac{1}{3I^2}\left[J\left(3IK-2J^2\right)+2\left(J^2-IK\right)^{3/2}\right],\\q_l=&\frac{1}{3I^2}\left[J\left(3IK-2J^2\right)-2\left(J^2-IK\right)^{3/2}\right],\end{aligned}\tag{36}$$

The condition providing the existence of the upper and lower buckling loads is

$$J^2-IK>0.\tag{37}$$

If ES-FGM cylindrical shells only subjects to axial compressive loads, substituting $q = 0, N_{x0} = -h.P_x$ into Eq. (33), obtains

$$P_x = \left(\frac{-1}{h\alpha^2}\right)\left(H_2.W^2 + H_1.W + H_0\right). \tag{38}$$

in which

$$\begin{aligned} H_0 &= \left[\alpha^4 B^*_{21} + \alpha^2\beta^2\left(B^*_{11} + B^*_{22} - 2B^*_{66}\right) + \beta^4 B^*_{12} - \frac{\alpha^2}{R}\right] L_3 + \\ &\quad + \left[\alpha^3 D^*_{11} + \alpha\beta^2\left(D^*_{21} + 2D^*_{66}\right)\right] L_4 + \left[\beta^3 D^*_{22} + \alpha^2\beta\left(D^*_{12} + 2D^*_{66}\right)\right] L_5 - K_1 - \left(\alpha^2 + \beta^2\right) K_2, \\ H_1 &= \left(16\alpha^4 B^*_{21} L_1 + 16\beta^4 B^*_{12} L_2 - 2\alpha^2\beta^2 L_3 - \frac{4\alpha^2}{R} L_1 - 8\alpha^3 D^*_{11} L_6 - 8\beta^3 D^*_{22} L_7\right)\left(\frac{-16}{3\alpha\beta L\pi R}\delta_m\delta_n\right), \\ H_2 &= -2\alpha^2\beta^2\left(L_1 + L_2\right). \end{aligned} \tag{39}$$

Taking $W \to 0$, Eq. (38) gives the upper buckling load as

$$P_{upper} = \left(\frac{-1}{h\alpha^2}\right) H_0. \tag{40}$$

The lower buckling load can be obtained from Eq. (38) by using the condition $\dfrac{dP_x}{dW} = 0$ leads to $W_* = \dfrac{-H_1}{2H_2}$ and obtains

$$P_{lower} = P_x\left(W_*\right) = \left(\frac{-1}{h\alpha^2}\right)\left(H_0 - \frac{H_1^2}{4H_2}\right). \tag{41}$$

4. NUMERICAL RESULTS AND DISCUSSION

4.1. Comparison results

As part of the validation of the present approach, a simple supported un-stiffened FGM cylindrical shell without elastic foundations under axial compressive load is considered. The geometrical and material properties of the cylindrical shell are taken by [15] $L/R = 2$; $E_c = 168.08 \times 10^9$ Pa; $E_m = 105.69 \times 10^9$ Pa; ν =0.3, and k and R/h change. The buckling load of static-axial loaded FGM cylindrical shells $P_{scr} = P_{dcr}/\tau_{cr}$ in which

Table 1. Comparisons with results of [15] for un-stiffened FGM cylindrical shells without elastic foundations under axial compressive load

		Huang and Han	Present	Difference (%)
Critical load versus k				
$R/h = 500$	$k = 0.2$	189.262 (2,11)[a]	189.166 (3,13)	0.051
	$k = 1.0$	164.352 (2,11)	164.248 (3,13)	0.063
	$k = 5.0$	144.471 (2,11)	144.123 (3,13)	0.241
Critical load versus R/h				
$k = 0.2$	$R/h = 400$	236.578 (5,15)	236.245 (19,14)	0.141
	$R/h = 600$	157.984 (3,14)	157.558 (22,19)	0.270
	$R/h = 800$	118.898 (2,12)	118.1658 (33,1)	0.616

[a] Buckling mode (m, n).

the non-dimensional parameter τ_{cr} is the critical parameter and P_{dcr} is the corresponding dynamic buckling load, is calculated by Huang and Han [15] and P_{upper} is given by Eq. (40) in this paper. The comparison results are given in Tab. 1. It is seen that the present results are in good agreement to those from the reference [5].

4.2. ES-FGM cylindrical shells surrounded by elastic foundations

In this section the above formulations are used to analyze the effects of input parameters on buckling and post-buckling behavior of cylindrical shells. The geometric properties of shells are $h = 0.006$m, $R/h = 100$, $L/R = 2$, $h_1 = h_2 = 0.006$ m, $b_1 = b_2 = 0.003$ m and $d_1 = 2\pi R/n_1$ m, $d_2 = L/n_2$ m. The material properties are $E_c = 380\times10^9$ Pa, $E_m = 70\times10^9$ Pa, $\nu = 0.3$.

Table 2. Critical buckling compressive load for different types of stiffeners ($k = 1$)

$P_{upper\,cr}$(MPa)	Inside stiffeners	Outside stiffeners
Without stiffeners	1244.0685 (12,2)	1244.0685 (12,2)
Longitudinal stiffeners ($n_1 = 26$)	1251.1232 (2,7)	1257.5814 (2,7)
Circumferential stiffeners ($n_2 = 26$)	1250.7971 (9,8)	1257.1162 (12,1)
Orthogonal stiffeners ($n_1 = n_2 = 13$)	1305.0626 (7,9)	1279.5732 (12,1)

^{a} Buckling mode (m, n).

Tab. 2 shows that the critical buckling loads of FG cylindrical shells without foundations only attached by x-stiffener or by y-stiffener are close each other. But, the combination of longitudinal and circumferential stiffeners has strongly effect on the stability of cylindrical shells. The critical load in this case is biggest, but the critical load of cylindrical shells attached by circumferential stiffeners is smallest, for stiffened cylindrical shells. As results in Tab. 2, it can be seen that the critical buckling load of stiffened cylindrical shells is greater than one of un-stiffened cylindrical shells. It is reasonable because the present of stiffeners makes cylindrical shells to become more rigid.

Table 3. Critical buckling compressive loads (MPa) for different types of foundation parameters ($k = 1$)

Foundation parameters	$K_1 = K_2 = 0$	$K_1 = 2.5\times10^8$ N/m^3, K$_2 = 5\times10^5$ N/m	$K_1 = 0$, $K_2 = 0$	$K_1 = 2.5\times10^8$ N/m^3, $K_2 = 5\times10^5$ N/m
$P_{upper\,cr}$	1244.0685 (12,2)	1286.2857(12,2)	1327.7614 (12,1)	1369.9786 (12,1)

^{a} Buckling mode (m, n).

Tab. 3 shows the effect of the foundation on the critical buckling loads of FGM cylindrical shells without stiffeners in which the foundation parameters are $K_1 = 2.5\times10^8$ N/m^3, $K_2 = 5\times10^5$ N/m. The critical load using two foundation parameters is biggest, whereas the critical load without foundations is smallest. This difference is considerable.

For example $P_{upper\,cr} = 1369.9786$ MPa for shell with two foundation parameters is great than $P_{upper\,cr} = 1244.0685$ MPa for shell without about 9.2%.

Tab. 4 shows the effect of both foundations and stiffeners on the critical buckling loads of FGM cylindrical shells. The number of stiffeners is 26 in all cases. If cylindrical shells have the same value of foundation parameters, the critical load is biggest for longitudinal stiffeners, but the critical load is smallest for circumferential stiffeners. The case of two foundation parameters is biggest, the case of the first foundation parameter is smallest for the same type of stiffener.

Table 4. Critical buckling compressive loads (MPa) for different types of foundation parameters and stiffeners ($k = 1$)

$P_{upper\,cr}$(MPa)	$K_1 = 2.5\times10^8$ N/m^3, $K_2 = 0$	$K_1 = 0$, $K_2 = 5\times10^5$ N/m	$K_1 = 2.5\times10^8$ N/m^3, $K_2 = 5\times10^5$ N/m
Longitudinal stiffeners ($n_1 = 26$)	1432.0105 (8,9)	1451.0503 (7,9)	1558.0887 (8,9)
Circumferential stiffeners ($n_2 = 26$)	1309.8784 (11,7)	1351.9671 (10,7)	1406.1543 (11,6)
Orthogonal stiffeners ($n_1 = n_2 = 13$)	1389.0893 (9,8)	1424.0553 (9,8)	1495.6795 (10,7)

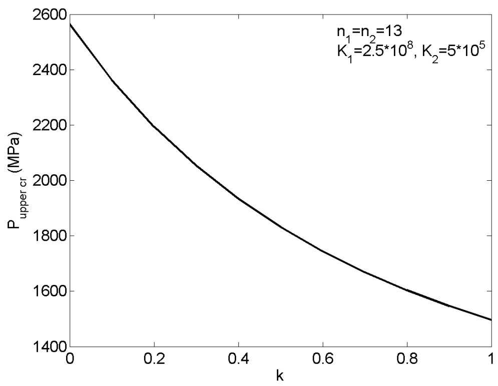

Fig. 2. Effect of volume fraction index on the nonlinear response of ES-FGM cylindrical shells under axial compressive load

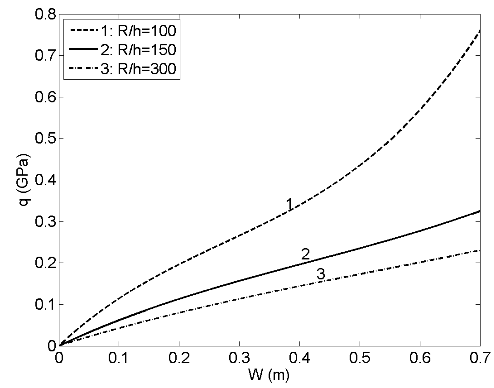

Fig. 3. Effect of radius-to-thickness ratio on the nonlinear response of ES-FGM cylindrical shells under external pressure

Fig. 2 shows the effect of material index k on the stability of inside-stiffened FG cylindrical shells. As can be seen, the critical buckling compressive loads decrease when the value of k increases.

In Fig. 3, the effects of radius-to-thickness ratios are focused on with $(m, n) = (1, 1)$, $k = 1$. Three values of R/h are 100, 150 and 300. As can be seen that the post-buckling load-deflection curves become lower when the values of R/h increase.

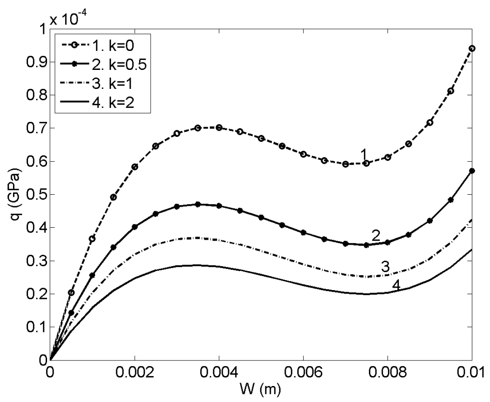

Fig. 4. Effect of volume fraction index on the nonlinear response of un-stiffened FG cylindrical shells under external pressure without elastic foundations

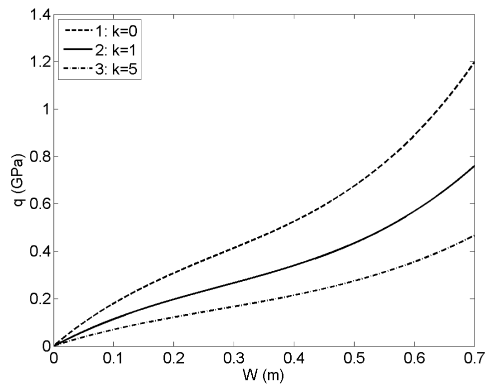

Fig. 5. Effect of volume fraction index on the nonlinear response of inside-stiffened FG cylindrical shells under external pressure with elastic foundations

Figs. 4 and 5 show the effect of volume fraction index on the nonlinear response of FG cylindrical shells under external pressure. Fig. 4 is plotted with $k = 0, 0.5, 1$ and 5 and $(m, n) = (1, 3)$, $L = 2$ m, $L/R = 5, R/h = 100$ for cylindrical shells without both stiffeners and foundations. Fig. 5 is plotted with $k = 0, 1$ and 5, $(m, n) = (1, 1)$, $h = 0.006$ m, $L/R = 2, R/h = 100$ for cylindrical shells with orthogonal stiffeners and two-parameter foundation. As can be seen that the post-buckling load-deflection curves become lower when the values of k increase, i.e. the load carrying capacity of structures decreases with the greater percentage of metal.

5. CONCLUSIONS

This paper presents an analytical solution to investigate the buckling and post-buckling behavior of ES-FGM cylindrical shells surrounded by an elastic medium subjected to mechanical compressive loads and external pressures. Theoretical formulations are based on the smeared stiffeners technique and the first-order shear deformation theory. The analytical expressions to determine the static critical buckling load and analyze the post-buckling load-deflection are obtained. Numerical results shows the effects of stiffeners, geometrical parameters and elastic foundations on the buckling and post-buckling response of ES-FGM cylindrical shells. Some following remarks are deduced from the present results:

a. The stiffeners enhance the stability of cylindrical shells. Particularly, the combination of longitudinal and circumferential stiffeners has strongly effect on the stability of shells. The critical load in this case is biggest.

b. The foundation parameters affects strongly critical buckling load. Especially, the critical buckling load corresponding to the presence of the both foundation parameters K_1 and K_2 is biggest.

c. The loading carrying capacity of shell is reduced considerably when R/h ratio or volume fraction index k increases.

ACKNOWLEDGEMENT

This research is funded by Vietnam National Foundation for Science and Technology Development (NAFOSTED) under Grant number 107.02-2013.02 and the project No.TN-14. The authors are grateful for the financial support.

REFERENCES

[1] Bagherizadeh E, Kiani Y, Eslami MR, Mechanical buckling of functionally graded material cylindrical shells surrounded by Pasternak elastic foundation, *Compos Struct*, **93**, (2011), pp. 3063–3071.

[2] Shen HS, Wang H, Thermal post-buckling of functionally graded fiber reinforced composite cylindrical shells surrounded by an elastic medium, *Compos Struct*, **102**, (2013), pp. 250–260.

[3] Shen HS, Post-buckling of shear deformable FGM cylindrical shells surrounded by an elastic medium, *International Journal of Mechanical Sciences*, **51**, (2009), pp. 372–383.

[4] Shen HS, Jie Yang, Sritawat Kitipornchai, Post-buckling of internal pressure loaded FGM cylindrical shells surrounded by an elastic medium, *European Journal of Mechanics - A/Solids*, **29**, (2010), pp. 448–460.

[5] Sofiyev AH, Kuruoglu N, Torsional vibration and buckling of the cylindrical shell with functionally graded coatings surrounded by an elastic medium, *Compos Part B*, **45**, (2013), pp. 1133–1142.

[6] Bich DH, Nam VH, Phuong NT, Nonlinear post-buckling of eccentrically stiffened functionally graded plates and shallow shells, *Vietnam J Mech*, **33** (3), (2011), pp. 132–147.

[7] Bich DH, Dung DV, Nam VH, Nonlinear dynamical analysis of eccentrically stiffened functionally graded cylindrical panels, *Compos Struct*, **94**, (2012), pp. 2465–2473.

[8] Bich DH, Dung DV, Nam VH, Nonlinear dynamic analysis of eccentrically stiffened imperfect functionally graded doubly curved thin shallow shells, *Compos Struct*, **96**, (2013), pp. 384–395.

[9] Najafizadeh MM, Hasani A, Khazaeinejad P, Mechanical stability of functionally graded stiffened cylindrical shells, *Appl Math Model*, **33**, (2009), pp. 1151–1157.

[10] Dung DV, Hoa LK, Research on nonlinear torsional buckling and post-buckling of eccentrically stiffened functionally graded thin circular cylindrical shells, *Compos Part B*, **51**, (2013), pp. 300–309.

[11] Dung DV, Hoa LK, Nonlinear buckling and post-buckling analysis of eccentrically stiffened functionally graded circular cylindrical shells under external pressure, *Thin Walled Struct*, **63**, (2013), pp. 117–124.

[12] Reddy JN, *Mechanics of laminated composite plates and shells: Theory and Analysis*, CRC Press LLC, (2004).

[13] Brush DO, Almroth BO, *Buckling of bars, plates and shells*, Mc Graw-Hill, New York, (1975).

[14] Peng LX, Kitipornchai S, Liew KM, Analysis of rectangular stiffened plates under uniform lateral load based on FSDT and element-free Galerkin's method, *Int J Mech Sci*, **47** (2005), pp. 251–276.

[15] Huang H, Han Q, Nonlinear dynamic buckling of functionally graded cylindrical shells subjected to time dependent axial load, *Compos Struct*, **92**, (2010), pp. 593–598.

Received June 18, 2013

APPENDIX I

$$\Delta = \left(A_{11} + \frac{E_{sx}A_1}{d_1}\right)\left(A_{22} + \frac{E_{sy}A_2}{d_2}\right) - A_{12}^2,$$

$$A_{11}^* = \frac{1}{\Delta}\left(A_{11} + \frac{E_{sx}A_1}{d_1}\right), \quad A_{22}^* = \frac{1}{\Delta}\left(A_{22} + \frac{E_{sy}A_2}{d_2}\right), \quad A_{12}^* = \frac{A_{12}}{\Delta}, \quad A_{66}^* = \frac{1}{A_{66}},$$

$$B_{11}^* = A_{22}^*\left(B_{11} + C_1\right) - A_{12}^* B_{12}, \quad B_{22}^* = A_{11}^*\left(B_{22} + C_2\right) - A_{12}^* B_{12},$$

$$B_{12}^* = A_{22}^* B_{12} - A_{12}^*\left(B_{22} + C_2\right), \quad B_{21}^* = A_{11}^* B_{12} - A_{12}^*\left(B_{11} + C_1\right), \quad B_{66}^* = \frac{B_{66}}{A_{66}},$$

$$\begin{aligned}
D_{11}^* &= D_{11} + \frac{E_{sx}I_1}{d_1} - B_{11}^*\left(B_{11} + C_1\right) - B_{21}^* B_{12},\\
D_{22}^* &= D_{22} + \frac{E_{sy}I_2}{d_2} - B_{22}^*\left(B_{22} + C_2\right) - B_{12}^* B_{12},\\
D_{12}^* &= D_{12} - B_{12}^*\left(B_{11} + C_1\right) - B_{22}^* B_{12},\\
D_{21}^* &= D_{12} - B_{21}^*\left(B_{22} + C_2\right) - B_{11}^* B_{12},\\
D_{66}^* &= D_{66} - B_{66}^* B_{66}.
\end{aligned}$$

APPENDIX II

$$\begin{aligned}
L_1 &= \frac{4\alpha^2 D_{11}^* + A_{44}}{A_{11}^*\left(4\alpha^2 D_{11}^* + A_{44}\right) + 4\alpha^2 B_{21}^{*2}} \cdot \frac{\beta^2}{32\alpha^2},\\
L_2 &= \frac{4\beta^2 D_{22}^* + A_{55}}{A_{22}^*\left(4\beta^2 D_{22}^* + A_{55}\right) + 4\beta^2 B_{12}^{*2}} \cdot \frac{\alpha^2}{32\beta^2},\\
L_3 &= \frac{\left(A_{44}a_{22}\alpha - A_{55}a_{12}\beta\right)a_{13} + \left(A_{55}a_{11}\beta - A_{44}a_{21}\alpha\right)a_{23} + \dfrac{D^*}{R}\alpha^2}{D^*\left[\alpha^4 A_{11}^* + \alpha^2\beta^2\left(A_{66}^* - 2A_{12}^*\right) + \beta^4 A_{22}^*\right] + \left(a_{13}a_{22} - a_{12}a_{23}\right)a_{13} + \left(a_{11}a_{23} - a_{21}a_{13}\right)a_{23}},\\
L_4 &= \frac{L_3}{D^*}\left(a_{13}a_{22} - a_{12}a_{23}\right) - \frac{A_{44}a_{22}\alpha - A_{55}a_{12}\beta}{D^*},\\
L_5 &= \frac{L_3}{D^*}\left(a_{11}a_{23} - a_{21}a_{13}\right) - \frac{A_{55}a_{11}\beta - A_{44}a_{21}\alpha}{D^*},\\
L_6 &= \frac{8\alpha^3 B_{21}^*}{4\alpha^2 D_{11}^* + A_{44}} \cdot L_1, \quad L_7 = \frac{8\beta^3 B_{12}^*}{4\beta^2 D_{22}^* + A_{55}} \cdot L_2,
\end{aligned}$$

in which

$$\begin{aligned}
&a_{11} = \alpha^2 D_{11}^* + \beta^2 D_{66}^* + A_{44}, && a_{22} = \beta^2 D_{22}^* + \alpha^2 D_{66}^* + A_{55},\\
&a_{12} = \alpha\beta\left(D_{12}^* + D_{66}^*\right), && a_{21} = \alpha\beta\left(D_{21}^* + D_{66}^*\right),\\
&a_{13} = -\left[\alpha^3 B_{21}^* + \alpha\beta^2\left(B_{11}^* - B_{66}^*\right)\right], && a_{23} = -\left[\beta^3 B_{12}^* + \alpha^2\beta\left(B_{22}^* - B_{66}^*\right)\right],\\
&D^* = a_{11}a_{22} - a_{12}a_{21}.
\end{aligned}$$

VIETNAM ACADEMY OF SCIENCE AND TECHNOLOGY
VIETNAM JOURNAL OF MECHANICS VOLUME 35, N. 4, 2013

CONTENTS